

Cambridge University Press & Assessment

978-1-605-11471-2 — Oxide Semiconductors and Thin Films

Edited by André Schleife , Martin Allen , Craig B. Arnold , Steven M. Durbin , Nini Pryds , Christof W. Schneider , Tim Veal

Excerpt

[More Information](#)

ZnO and Related Materials

Mat. Res. Soc. Symp. Proc. Vol. 1494 © 2012 Materials Research Society

DOI: 10.1557/opl.2012.1574

Acceptor Dopants in Bulk and Nanoscale ZnO

Matthew D. McCluskey,¹ Marianne C. Tarun,¹ and Samuel T. Teklemichael¹

¹Department of Physics and Astronomy, Washington State University
Pullman, WA 99164-2814, U.S.A.

ABSTRACT

Zinc oxide (ZnO) is a semiconductor that emits bright UV light, with little wasted heat. This intrinsic feature makes it a promising material for energy-efficient white lighting, nanolasers, and other optical applications. For devices to be competitive, however, it is necessary to develop reliable *p*-type doping. Although substitutional nitrogen has been considered as a potential *p*-type dopant for ZnO, recent theoretical and experimental work suggests that nitrogen is a deep acceptor and will not lead to *p*-type conductivity. In nitrogen-doped samples, a red photoluminescence (PL) band is correlated with the presence of deep nitrogen acceptors. PL excitation (PLE) measurements show an absorption threshold of 2.26 eV, in good agreement with theory. The results of these studies seem to rule out group-V elements as shallow acceptors in ZnO, contradicting numerous reports in the literature. Optical studies on ZnO nanocrystals show some intriguing leads. At liquid-helium temperatures, a series of sharp IR absorption peaks arise from an unknown acceptor impurity. The data are consistent with a hydrogenic acceptor 0.46 eV above the valence band edge. While this binding energy is still too deep for many practical applications, it represents a significant improvement over the 1.4–1.5 eV binding energy for nitrogen acceptors. Nanocrystals present another twist. Due to their high surface-to-volume ratio, surface states are especially important. In our model, the 0.46 eV level is shallow with respect to the surface valence band, raising the possibility of surface hole conduction.

INTRODUCTION

ZnO is an electronic material with desirable properties for a range of energy applications.¹ ZnO is a wide band gap (3.4 eV) semiconductor that emits light in the near-UV region of the spectrum. The high efficiency of the emission, thanks in part to stable excitons at room temperature,² makes ZnO a strong candidate for efficient solid-state white lighting. Reports of stimulated emission in ZnO nanowires^{3,4} and multicrystallite thin films^{5,6} suggest the feasibility of UV lasers made from this material. ZnO is already used as a transparent conductor⁷ in solar cells, a UV-absorbing component in sunscreens,⁸ and the active material in varistors.⁹ Researchers have also fabricated transparent transistors, invisible devices that could find widespread use in products such as liquid-crystal displays.¹⁰

Besides its fundamental optical and electrical properties, ZnO has other benefits that could make it a dominant material for energy applications. In contrast to GaN, large single crystals can be grown routinely.¹¹ ZnO is relatively benign environmentally and is actually used as a dietary supplement in animal feed.¹² From an economic perspective, the low cost of zinc versus indium provides an advantage over indium tin oxide for use as a transparent conductor.⁷

Despite these advantages, the lack of fundamental knowledge about dopants and defects presents an obstacle to the development of practical devices. Reliable *p*-type doping, required for high-performance transistors, lasers, or light-emitting diodes (LEDs), has been elusive.¹³ As reviewed by McCluskey and Jokela,¹⁴ the scientific literature contains numerous reports that

nitrogen doping can produce *p*-type ZnO. However, Look and Chafin¹⁵ and Bierwagen *et al.*¹⁶ have pointed out the difficulty in determining carrier type from Hall-effect measurements on low-mobility samples.

More recently, Lyons, Janotti, and Van de Walle¹⁷ calculated the properties of substitutional nitrogen in ZnO using density functional theory (DFT) with hybrid functionals. Their calculations show that nitrogen is a *deep* acceptor, with the acceptor level 1.3 eV above the valence-band maximum. Lany and Zunger,¹⁸ using generalized Koopmans DFT, obtained an even deeper level. Such a deep level would yield an insignificant hole concentration at room temperature.

In our experimental work,¹⁹ we provided evidence that nitrogen is indeed a deep acceptor and therefore cannot produce *p*-type ZnO. A broad PL emission band near 1.7 eV, with an excitation onset of ~2.2 eV, was observed, in agreement with the deep-acceptor model¹⁷ of the nitrogen defect. The deep level can be explained by considering the low energy of the ZnO valence band relative to the vacuum level. In our “universal acceptor model,” we hypothesize that acceptor levels are roughly constant, irrespective of the host semiconductor. As shown in Fig. 1, these levels tend to be much higher than the ZnO valence band and therefore are “deep.” This intrinsic feature of ZnO and other oxide semiconductors, which stems from the large electronegativity of oxygen, will prove a formidable challenge to *p*-type doping.

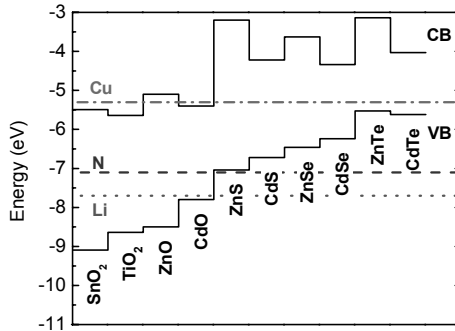


Figure 1. Proposed universal acceptor levels for copper, nitrogen, and lithium. Valence-band (VB) offsets are from theory^{20,21} and experiment,²² while conduction band (CB) minima are from the experimental band gaps. Energy values are relative to the vacuum level.²³ Levels for copper,²⁴ nitrogen,¹⁷ and lithium²⁵ acceptors are their values in ZnO and are assumed to be constant relative to vacuum.

EXPERIMENT

Bulk single crystals were grown via seeded chemical vapor transport in an ammonia (NH_3) ambient, which provides nitrogen and hydrogen dopants.²⁶ An undoped reference sample was obtained by growing the crystal in an argon ambient. ZnO nanopowder was purchased from Sigma-Aldrich. Scanning electron microscopy (SEM) indicated that the particles have an average diameter of ~ 90 nm. The particles were pressed into pellets 7 mm in diameter with a thickness of 0.25 mm.

Infrared spectroscopy was performed using a Bomem DA8 vacuum Fourier transform infrared (FTIR) spectrometer with a global light source, a KBr beamsplitter, and a liquid-nitrogen-cooled indium antimonide (InSb) detector. PL and PLE measurements were obtained using a JY-Horiba FluoroLog-3 spectrofluorometer equipped with double-grating excitation and emission monochromators (1200 grooves/mm; 2.1 nm/mm dispersion) and an R928P photomultiplier tube (PMT). The excitation source was a 450-W xenon CW lamp. An instrumental correction was performed to correct for the wavelength-dependent PMT response, grating efficiencies, and the variation in output intensity from the lamp.

DISCUSSION

Nitrogen in bulk ZnO

Figure 2 shows the red PL band (~ 1.7 eV) from N-doped and undoped samples. The spectra were obtained with excitation energy of 2.53 eV at room temperature. The inset shows the IR absorption peak of the N-H complex. The samples were annealed in O_2 at 775°C to dissociate some of the N-H bonds and activate isolated nitrogen acceptors. The intensity of the red PL band is proportional to the concentration of activated N acceptors. The N-doped sample clearly shows a much higher intensity.

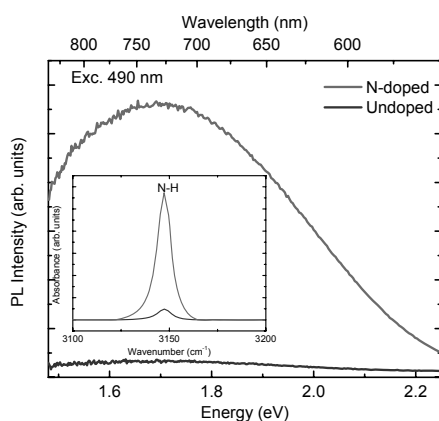


Figure 2. Red PL band from N-doped and undoped ZnO samples, at an excitation energy of 490 nm (2.53 eV). Inset: IR absorption peak of the N-H complex from the two respective samples.

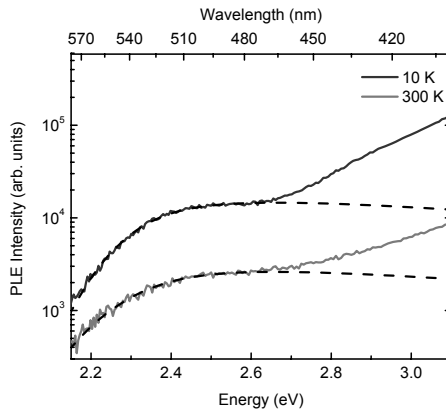


Figure 3. PLE spectrum of the red band (720 nm) of N-doped sample at 10 K and 300 K. Fits from the model²⁷, with parameters $E_{\text{opt}} = 2.26$ eV and $\Delta E = 0.14$ eV for 10 K and $E_{\text{opt}} = 2.24$ eV and $\Delta E = 0.18$ eV for 300 K, are shown by the broken lines.

In Fig. 3, the PLE spectrum for the red band from the N-doped sample was obtained by monitoring the intensity of the red emission at 720 nm as a function of excitation energy. The PLE signal is proportional to the absorption cross section of the N_O^- defect. An explicit formula for the absorption of deep levels was obtained by Jaros.²⁷ In that model, the key parameters are E_{opt} , the vertical transition energy from the deep level to the conduction band minimum, and ΔE , the broadening due to vibrational overlap between the initial and final states. Other parameters, which do not affect the absorption onset significantly, were obtained from Ref. 28. As shown in Fig. 3, the model produces good fits to the PLE spectrum for photon energies below 2.6 eV. The model parameters are $E_{\text{opt}} = 2.26$ eV and $\Delta E = 0.14$ eV for 10 K, and $E_{\text{opt}} = 2.24$ eV and $\Delta E = 0.18$ eV for 300 K. The increase above 2.6 eV may be due to other defect levels or band-tail states.

These results are consistent with the configuration coordinate diagram for optical transitions based on the nitrogen deep-acceptor model.¹⁷ Specifically, we find a Stokes shift of $2.24 - 1.68 = 0.56$ eV at room temperature. Assuming that the Frank-Condon shift is roughly half this value, we estimate that the nitrogen acceptor level is 1.9–2.0 eV below the conduction-band minimum. This places the acceptor level 1.4–1.5 eV above the valence-band maximum, in good agreement with theory.

The peak energy position of the red band as a function of temperature is shown in Fig. 4. At low temperatures, a band in the near-IR (1.5 eV) grows and dominates, leading to an apparent shift in the PL peak. The origin of this near-IR band is not known. One possibility is that N-H has a donor level in the gap.²⁹ The transition of an electron to this donor level may yield a PL peak.

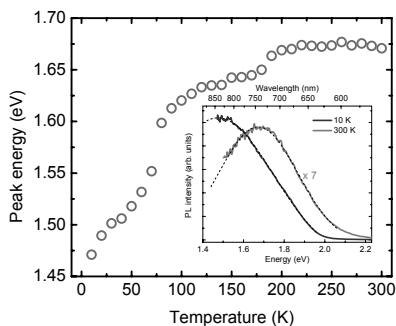


Figure 4. Peak energy position of the red band as a function of temperature. Inset: PL spectra at 10 K and 300 K, respectively. Gaussian fits are shown by the broken lines.

Acceptors in ZnO nanocrystals

Previous work^{30,31} showed a low temperature (10 K) series of IR absorption peaks, in the energy range of 0.425–0.457 eV, for “as-grown” ZnO nanoparticles of average diameter ~ 20 nm. The result was characteristic of a hydrogenic acceptor spectrum with a hole binding energy of 0.4–0.5 eV. Although the identity of the acceptor was not determined, electron paramagnetic resonance measurements suggested that it may be a vacancy complex. In this work, as received ZnO nanoparticles from Sigma-Aldrich with larger diameter (~ 90 nm) showed similar results as the as-grown sample.

Figure 5 shows strong IR absorption spectrum for the as-received (Sigma-Aldrich) ZnO nanoparticles, consistent with previous work.^{30,31} The IR absorption spectrum was calculated using $\text{absorbance} = \log_{10}(I_R/I)$, where I_R and I are the transmission spectra for no sample (blank) and an as-received sample, respectively. A quadratic baseline was then subtracted from the absorbance spectrum. The IR absorption peaks disappear (not shown here) after exposure to formic acid (HCOOH) vapor, consistent with electrical compensation of the acceptor by the formate ion. This observation also agrees with our previous results on as-grown ZnO nanocrystals.³²

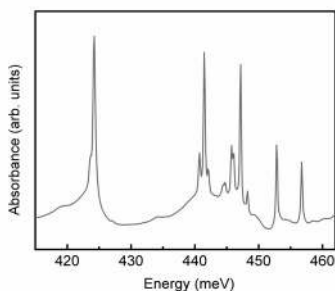


Figure 5. Low temperature (10 K) IR spectrum of as-received ZnO nanocrystals, showing electronic transitions.

Figure 6 shows the temperature dependence of the integrated area, for one of the IR peaks, indicating consistent results upon cooling and warming the sample. The inset shows the IR peak, corresponding to a hydrogenic excited state, decreasing with temperature. The disappearance of the peak at high temperatures is evidence of thermal ionization of the acceptors. The solid line is a fit according to a Boltzmann distribution function,

$$\alpha(T) = \alpha_0 / [1 + g \exp(-\Delta E/k_B T)], \quad (1)$$

where α_0 is a constant, g is a degeneracy factor, ΔE is an activation energy, k_B is the Boltzmann constant and T is temperature (K). The fit yields $\Delta E = 0.09 \pm 0.01$ eV and $g = 132 \pm 94$. This result is consistent with the previous report on the as-grown ZnO nanoparticles, $\Delta E = 0.08$ eV.³¹

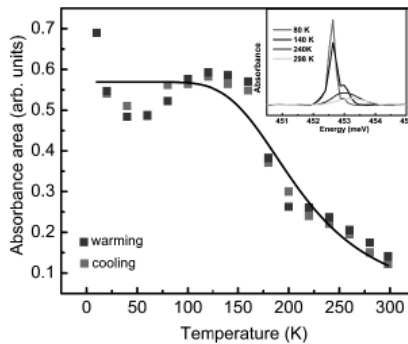


Figure 6. IR absorbance area of an acceptor excited state peak upon cooling and warming of the sample. The solid line is a fit to the Boltzmann distribution function [Eq. (1)]. Inset: IR absorption spectra of an acceptor peak, showing a decrease with temperature.

The activation energy ΔE is much lower than the hole binding energy of 0.46 eV. We proposed that the holes are thermally excited from the acceptor ground state to a band of surface states that lay 0.38 eV above the valence-band maximum.³¹ This model is qualitatively consistent with *ab initio* calculations that predict the existence of surface states 0.5 eV above the valence-band maximum.³³ According to our model, the acceptor is deep (0.46 eV) with respect to the bulk valence band but shallow (0.08 eV) with respect to the surface states.

Figure 7 shows a low-temperature (10 K) PL emission spectrum at an excitation wavelength of 325 nm, for the as-received ZnO nanocrystals. We observed a broad green emission band centered around 524 nm (2.37 eV), unlike the as-grown sample which showed a broad red luminescence. In general, surface states may involve defects and impurities. Hydroxides on the surface of ZnO nanocrystals,³⁴ for example, have been correlated with green emission.³⁵ The previously mentioned surface states, calculated to be 0.5 eV above the valence band, arise from oxygen-deficient surfaces.³³ However, there is also theoretical evidence that the surface states may be intrinsic. Calculations by Kresse *et al.*³⁶ show that valence-band and conduction-band surface states originate from the O-terminated and Zn-terminated *c*-face ZnO surfaces, respectively.

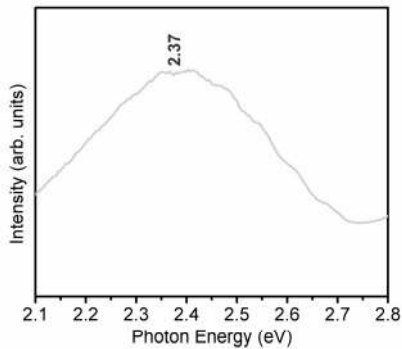


Figure 7. Low temperature (10 K) PL emission spectrum of ZnO nanocrystals at an excitation wavelength of 325 nm, showing green emission at 2.37 eV.

Figure 8 shows a low temperature (10 K) PL spectrum of the as-received ZnO nanocrystals under an excitation wavelength of 325 nm. Peaks in the near-band-gap range of 3.18 eV – 3.35 eV have previously been attributed to bound excitons and their phonon replicas. The PL peak at 3.36 eV is due to the neutral donor bound exciton (D^0, X).³⁷ We noticed this emission peak is blue shifted compared to the previous PL emission (3.35 eV) observed in the as-grown sample.³¹ Low temperature PL peaks at 3.31 and 3.22 eV have been attributed to the TO and TO + LO phonon replica of donor bound excitons.^{38, 39} Fonoberov *et al*⁴⁰ attributed the PL peak around 3.31 eV observed at low temperature ($T < 150$ K) in ZnO nanocrystals to acceptor bound excitons (A^0, X). They suggested that zinc vacancies or surface defects could act as acceptor impurities. Fallert *et al*⁴¹ assigned the same peak (around 3.31 eV), observed in ZnO powders at 5 K, to excitons bound to defect states at the particle surface. The PL peak at 3.22 eV, recorded at 4.2 K, has been assigned to donor-acceptor pair transitions involving a shallow donor and shallow acceptor.⁴² The emission peak at 3.17 eV could be compared with the previous emission peak observed at 3.18 eV in the as-grown ZnO nanocrystals. This PL peak could be due to LO phonon replica of the donor bound exciton.⁴³ The PL emission at 3.11 eV, not observed in the as-grown sample, could perhaps be due to a phonon replica of the donor bound exciton.

In our previous work on the as-grown ZnO nanocrystals,³¹ the 2.97 eV emission peak was attributed to the transition of a free electron to the neutral acceptor. In the present work, the observation of this emission peak on the as-received ZnO nanocrystals indicates consistent result. In the PL experiment, above-gap light excites electrons into the conduction band. Electrons then fall from the conduction-band minimum to the acceptor level, emitting a photon of energy $3.43 - 0.46 = 2.97$ eV. This PL peak supports the argument that ZnO nanocrystals contain acceptors with a hole binding energy of 0.46 eV.

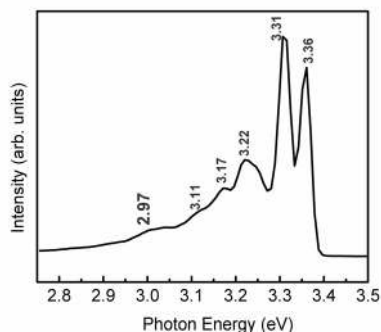


Figure 8. Low temperature (10 K) PL emission spectrum of ZnO nanocrystals at an excitation wavelength of 325 nm.

CONCLUSIONS

Our experimental evidence suggests that nitrogen is a deep acceptor in ZnO, with a hole ionization energy of 1.4–1.5 eV. The center shows a Stokes shift of 0.56 eV, consistent with large lattice relaxation. Clearly, such a deep acceptor is impractical for *p*-type doping. ZnO nanocrystals appear to contain an acceptor with a hole ionization energy of 0.46 eV. While the identity of this acceptor is unknown, we speculate that it could involve a zinc vacancy.

ACKNOWLEDGMENTS

The authors acknowledge helpful discussions with Leah Bergman, Evan Glaser, Eugene Haller, Stephan Lany, Chris Van de Walle, and Wladek Walukiewicz. Funding for this work was provided by the National Science Foundation Grant No. DMR-1004804 (MDM, MCT) and Department of Energy Grant No. DE-FG02-07ER46386 (STT).

REFERENCES

1. S.J. Pearton, D.P. Norton, K. Ip, Y.W. Heo, and T. Steiner, *Journ. Vacuum Sci. Tech B* **22**, 932 (2004).
2. D.C. Look, “Recent advances in ZnO materials and devices,” *Mater. Sci. Engin. B* **80**, 383 (2001).
3. M.H. Huang, S. Mao, H. Feick, H.Q. Yan, Y.Y. Wu, H. Kind, E. Weber, R. Russo, and P.D. Yang, *Science* **292**, 1897 (2001).
4. S. Chu, G. Wang, W. Zhou, Y. Lin, L. Chernyak, J. Zhao, J. Kong, L. Li, J. Ren and J. Liu, *Nature Nanotechnology* **6**, 506 (2011).
5. Z.K. Tang, G.K.L. Wong, P. Yu, M. Kawasaki, A. Ohtomo, H. Koinuma, and Y. Segawa, *Appl. Phys. Lett.* **72**, 3270 (1998).

6. P. Zu, Z.K. Tang, G.K.L. Wong, M. Kawasaki, A. Ohtomo, H. Koinuma, and Y. Segawa, *Solid State Commun.* **103**, 459 (1997).
7. T. Minami, *MRS Bulletin* **25** (8), 38 (2000).
8. G.P. Dransfield, *Radiat. Prot. Dosimetry* **91**, 271 (2000).
9. D.R. Clarke, *Journal of the American Ceramic Society* **82**, 485 (1999).
10. J.F. Wager, *Science* **300**, 1245 (2003).
11. J.M. Ntep, S.S. Hassani, A. Lusson, A. Tromson-Carli, D. Ballutaud, G. Didier, and R. Triboulet, *Journ. Crystal Growth* **207**, 30 (1999).
12. J.W. Smith, M.D. Tokach, R.D. Goodband, J.L. Nelssen, and B.T. Richert, *Journal of Animal Science* **75**, 1861 (1997).
13. S.J. Jokela and M.D. McCluskey, *Phys. Rev. B* **76**, 193201 (2007).
14. M.D. McCluskey and S.J. Jokela, *J. Appl. Phys.* **106**, 071101 (2009).
15. D.C. Look and B. Claflin, *Phys. Stat. Sol. (b)* **241**, 624 (2004).
16. O. Bierwagen, T. Ive, C.G. Van de Walle, and J.S. Speck, *Appl. Phys. Lett.* **93**, 242108 (2008).
17. J.L. Lyons, A. Janotti, and C.G. Van de Walle, *Appl. Phys. Lett.* **95**, 252105 (2009).
18. S. Lany and A. Zunger, *Phys. Rev. B* **81**, 205209 (2010).
19. M.C. Tarun, M. Zafar Iqbal, and M.D. McCluskey, *AIP Advances* **1**, 022105 (2011).
20. C.G. Van de Walle and J. Neugebauer, *Nature* **423**, 626 (2003).
21. Ç Kiliç and A. Zunger, *Appl. Phys. Lett.* **81**, 73 (2002).
22. J. Wang, X.-L. Liu, A.-L. Yang, G.-L. Zheng, S.-Y. Yang, H.-Y. Wei, Q.-S. Zhu, and Z.-G. Wang, *Appl. Phys. A* **103**, 1099 (2011).
23. R.L. Lichti, K.H. Chow, and S.F.J. Cox, *Phys. Rev. Lett.* **101**, 136403 (2008).
24. F.A. Selim, M.C. Tarun, D.E. Wall, L.A. Boatner, and M.D. McCluskey, *Appl. Phys. Lett.* **99**, 202109 (2011).
25. O.F. Schirmer and D. Zwingel, *Solid State Commun.* **8**, 1559 (1970).
26. S.J. Jokela, M.C. Tarun, and M.D. McCluskey, *Physica B* **404**, 4801 (2009).
27. M. Jaros, *Phys. Rev. B* **16**, 3694 (1977).
28. McCluskey, M.D., N.M. Johnson, C.G. Van de Walle, D.P. Bour, M. Kneissl, and W. Walukiewicz, *Phys. Rev. Lett.* **80**, 4008 (1998).
29. J.L. Lyons, A. Janotti, and C.G. Van de Walle, *Phys. Rev. Lett.* **108**, 156403 (2012).
30. S. T. Teklemichael, W. M. Hlaing Oo, M. D. McCluskey, E. D. Walter, and D. W. Hoyt, *Appl. Phys. Lett.* **98**, 232112 (2011).
31. S. T. Teklemichael and M. D. McCluskey, *Nanotechnology* **22**, 475703 (2011).
32. S. T. Teklemichael and M. D. McCluskey, *J. Phys. Chem. C* **116**, 17248 (2012).
33. J. D. Prades, A. Cirera, J. R. Morante, and A. Cornet, *Thin Solid Films* **515**, 8670 (2007).
34. H. Zhou, H. Alves, D.M. Hofmann, W. Kriegseis, B.K. Meyer, G. Kaczmarczyk, and A. Hoffmann, *Appl. Phys. Lett.* **80**, 210 (2002).
35. N.S. Norberg and D.R. Gamelin, *J. Phys. Chem. B* **109**, 20810 (2005).
36. G. Kresse, O. Dulub, and U. Diebold, *Phys. Rev. B* **68**, 245409 (2003).
37. D. C. Reynolds, D. C. Look, B. Jogai, C. W. Litton, T. C. Collins, W. Harsch, and G. Cantwell, *Phys. Rev. B* **57**, 12151 (1998).
38. T. Matsumoto, H. Kato, K. Miyamoto, M. Sano, E. A. Zhukov, and T. Yao, *Appl. Phys. Lett.* **81**, 1231 (2002).
39. Y. Zhang, B. Lin, X. Sun, and Z. Fu, *Appl. Phys. Lett.* **86**, 131910 (2005).